Predicting Atlantic Seasonal Hurricane Activity 6–11 Months in Advance

WILLIAM M. GRAY,* CHRISTOPHER W. LANDSEA,* PAUL W. MIELKE, JR.,† AND KENNETH J. BERRY†

Colorado State University, Fort Collins, Colorado

(Manuscript received 28 October 1991, in final form 30 April 1992)

ABSTRACT

A surprisingly strong long-range predictive signal exists for Atlantic-basin seasonal tropical cyclone activity. This predictive skill is related to two measures of West African rainfall in the prior year and to the phase of the stratospheric quasi-biennial oscillation of zonal winds at 30 mb and 50 mb, extrapolated ten months into the future. These predictors, both of which are available by 1 December, can be utilized to make skillful forecasts of Atlantic tropical cyclone activity in the following June–November season. Using jackknife methods to provide independent testing of datasets, it is found that these parameters can be used to forecast nearly half of the season-to-season variability for seven indices of Atlantic seasonal tropical cyclone activity as early as late November of the previous year.

1. Introduction

The Atlantic basin (including the Atlantic Ocean, Caribbean Sea, and Gulf of Mexico) experiences a larger variability of seasonal hurricane activity than does any other global hurricane basin (Gray 1985). Table 1 summarizes statistics on the year-to-year variability of various Atlantic seasonal tropical cyclone parameters. The number of hurricanes per season in recent years has ranged from 12 (1969), 11 (1950), and 9 (1955, 1980) to 2 (1982) and 3 (1957, 1962, 1972, 1983, 1987). This interannual variability suggests that large-scale climate factors acting on seasonal and longer-term time scales are involved and that some degree of seasonal predictability may be possible. Until recently, however, there has been no reliable objective method for predicting whether a forthcoming hurricane season was likely to be relatively active, inactive, or near normal.

Recent research (Gray 1984a,b, 1990b) indicates that there are seasonal hurricane predictive signals for the Atlantic basin from global and regional predictors that are available by 1 June (the beginning of the "official" hurricane season) and by 1 August (the beginning of the most active portion of the season). Similar highly skillful predictive relationships are generally not operative or are much weaker in other tropical cyclone basins (Chan 1991; Nicholls 1984) or in the middle latitudes (Livezey 1990). The five predictors utilized for these seasonal hurricane forecasts include two slowly varying global-scale climate factors: 1) the phase of the stratospheric quasi-biennial oscillation (QBO), and 2) the presence or absence of a moderate-to-strong El Niño event, and three persistent regional-scale factors: 3) 200-mb zonal wind; 4) sea level pressure anomalies in the Caribbean basin; and 5) the anticipated June–September rainfall in the western Sahel region of Africa. The importance of western Sahel rainfall to concurrent Atlantic-basin hurricane activity has only recently been recognized (Gray 1990a; Landsea 1991; Landsea and Gray 1992; Landsea et al. 1992). Incorporating this rainfall factor into seasonal tropical cyclone forecasts adds an additional degree of complexity in that it becomes necessary to correctly forecast western Sahel rainfall. However, the strength of the rainfall association demands that an estimate of the western Sahel rainfall be made.

Whereas the five predictors identified above are operative at the beginning of the Atlantic hurricane season, the purpose of this paper is to analyze the two extended-range predictors of Atlantic seasonal activity that are available 6–11 months in advance. These two extended-range predictors are 1) the forward-extrapolated (10 months) strength of stratospheric QBO zonal wind near 10°N latitude for September and 2) rainfall in West Africa that occurs prior to 1 December in the previous year. Currently, these are the only predictors for Atlantic tropical cyclones that have been identified to operate on such a long time scale.

This paper separately discusses each of the stratospheric QBO and West African–rainfall extended-range predictors and then performs jackknife statistical analyses to determine the degree of independent 6–11-

* Department of Atmospheric Science.
† Department of Statistics.

Corresponding author address: William M. Gray, Department of Atmospheric Science, Colorado State University, Fort Collins, CO 80523.

TABLE 1. Summary of statistics for Atlantic tropical cyclones and West African rainfall for 1950–1990. The numbered columns show yearly incidence of 1) named storms (NS), 2) named storm days (NSD), 3) hurricanes (H), 4) hurricane days (HD), 5) intense or category 3-4-5 hurricanes (IH) (Simpson 1974), 6) intense or category 3-4-5 hurricane days (IHD), 7) hurricane destruction potential (HDP), 8) precipitation anomaly expressed as standardized deviations for previous year August–November Gulf of Guinea (R_G) and 9) August–September precipitation in the western Sahel (R_S) of the previous year. An expanded discussion of these hurricane parameters is given in appendix A.

Year	NS 1	NSD 2	H 3	HD 4	IH 5	IHD 6	HDP 7	R_G 8	R_S 9	Year
1950	13	98	11	60	8	18.75	213	1.07	−0.14	1950
1951	10	58	8	36	5	8.25	120	−0.66	1.68	1951
1952	7	40	6	23	3	6.75	73	0.65	0.49	1952
1953	14	64	6	18	4	6.75	61	0.41	0.93	1953
1954	11	44	8	32	2	9.50	99	−0.16	0.20	1954
1955	12	82	9	47	6	17.25	171	0.64	0.60	1955
1956	8	30	4	13	2	2.75	40	0.41	1.00	1956
1957	8	38	3	21	2	6.50	71	−0.36	0.47	1957
1958	10	56	7	30	5	9.50	100	1.03	0.58	1958
1959	11	41	7	22	2	4.25	63	−0.74	1.45	1959
1960	7	30	4	18	2	11.00	80	0.12	0.25	1960
1961	11	71	8	48	7	24.50	183	1.05	0.23	1961
1962	5	22	3	11	1	0.50	26	−0.74	0.48	1962
1963	9	52	7	37	2	7.00	111	0.73	0.28	1963
1964	12	71	6	43	6	14.75	149	1.18	−0.12	1964
1965	6	40	4	27	1	7.50	78	−0.68	0.59	1965
1966	11	62	7	42	3	8.75	126	−0.17	0.75	1966
1967	8	58	6	36	1	5.75	102	−0.14	0.34	1967
1968	7	26	4	10	0	0.00	21	−0.51	0.72	1968
1969	17	84	12	40	5	6.75	114	1.28	−0.82	1969
1970	10	24	5	7	2	1.00	18	−0.31	0.38	1970
1971	13	63	6	29	1	1.00	65	−0.23	−0.45	1971
1972	4	21	3	6	0	0.00	14	−0.40	−0.19	1972
1973	7	33	4	10	1	0.25	24	−0.88	−1.10	1973
1974	7	32	4	14	2	4.25	46	0.43	−0.72	1974
1975	8	43	6	20	3	2.25	54	−0.08	−0.04	1975
1976	8	45	6	26	2	1.00	65	−0.55	0.06	1976
1977	6	14	5	7	1	1.00	18	−0.59	−0.50	1977
1978	11	40	5	14	2	3.50	40	−0.50	−0.75	1978
1979	8	44	5	22	2	5.75	73	−0.73	−0.36	1979
1980	11	60	9	38	2	7.25	126	0.55	−0.92	1980
1981	11	61	7	22	3	3.75	63	0.36	−0.34	1981
1982	5	16	2	6	1	1.25	18	−0.93	−0.44	1982
1983	4	14	3	4	1	0.25	8	−0.61	−0.90	1983
1984	12	51	5	18	1	0.75	42	−1.32	−1.24	1984
1985	11	51	7	21	3	4.00	61	0.04	−1.23	1985
1986	6	23	4	10	0	0.00	23	0.13	−0.51	1986
1987	7	37	3	5	1	0.50	11	−0.48	−0.01	1987
1988	12	47	5	24	3	8.00	81	1.37	−0.63	1988
1989	11	66	7	32	2	10.75	108	0.35	0.29	1989
1990	14	68	8	27	1	1.00	57	0.19	0.10	1990
Mean	9.34	46.83	5.83	23.80	2.46	5.71	73.56			
S.D.	2.98	20.03	2.21	13.62	1.90	5.60	49.29			
Coef. of Var.	0.32	0.43	0.38	0.57	0.77	0.98	0.67			

month forecast skill that is available from these two predictors.

2. QBO winds as a long-range predictor of hurricane activity

a. QBO variability

The easterly and westerly modes of stratospheric QBO zonal winds that circle the globe over the equatorial regions have a substantial influence on Atlantic tropical cyclone activity (Gray 1984a; Shapiro 1989). About twice as much intense-hurricane activity ($V_{max} \geq 50$ m s^{-1}) occurs during seasons when the stratospheric QBO winds at 50 mb (20-km level) are in the westerly anomaly mode. As illustrated in Figs. 1 and 2, the absolute values of the zonal vertical wind shear between 50 mb (20 km) and 30 mb (23 km) is relatively small in west-phase seasons. Table 2 shows the asso-

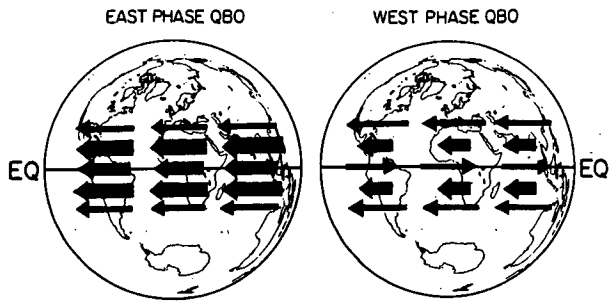

FIG. 1. Illustration of the two basic stratospheric QBO wind conditions that occur over the tropics at 50 mb and 30 mb during the summer season of both hemispheres. The left diagram shows conditions during the easterly phase of the QBO when easterly winds occur on the equator and winds at 10°N are strongly from the east. The right diagram, by contrast, shows conditions during the westerly phase of the QBO when stratospheric winds on the equator are from the west and winds at 10°N latitude are only weakly from the east. Hurricane activity is suppressed with conditions of the left diagram (east phase) and enhanced for conditions of the right diagrams. Length of arrows is proportional to wind speed.

ciations of forward-extrapolated (from November to September) stratospheric QBO zonal winds and Atlantic hurricane activity, particularly intense-hurricane activity. Note the large differences in the numbers of intense hurricane activity that occur between these two QBO stratified 15-yr groupings. Figure 3 shows the large differences in intense-hurricane tracks that are associated with these contrasting extrapolated QBO zonal-wind variations.

TABLE 2. Comparison of average seasonal hurricane activity in the 15 yr when the 10-month extrapolated sum of the September 50-mb QBO zonal wind near 10°N plus absolute values of the zonal wind shear to 30 mb was the lowest (westerly QBO phase) versus those 15 yr when this sum was the highest (easterly QBO phase) for the years 1950–1990.

	$[U_{50} - \lvert U_{50} - U_{30}\rvert]$		
	Lowest 15 yr westerly phase	Highest 15 yr easterly phase	Ratio lowest/ highest values
No. of hurricanes	7.07	4.80	1.47
No. of hurricane days	32.27	16.40	1.97
No. of intense hurricanes	3.53	1.67	2.12
No. of intense-hurricane days	8.30	2.97	2.80

The physical cause of these QBO-linked differences may be due to the contrasting stratospheric horizontal wind ventilation processes across the top of the hurricane, as illustrated in Fig. 2 and discussed by Gray (1988). During the east phase of the QBO, the absolute

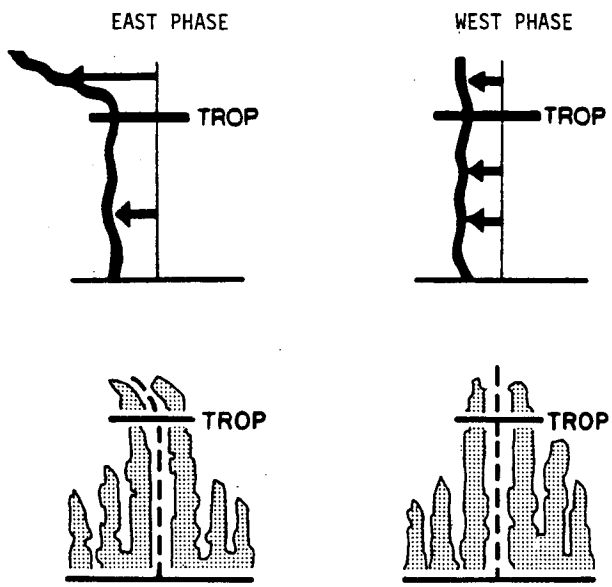

FIG. 2. Vertical cross-section illustration of the types of vertical wind shear and cloudiness associated with Atlantic tropical cyclones that extend through the tropopause (TROP) into the stratosphere. Conditions in the diagrams on the right are typical of west QBO periods, diagrams on the left of QBO easterly phase periods.

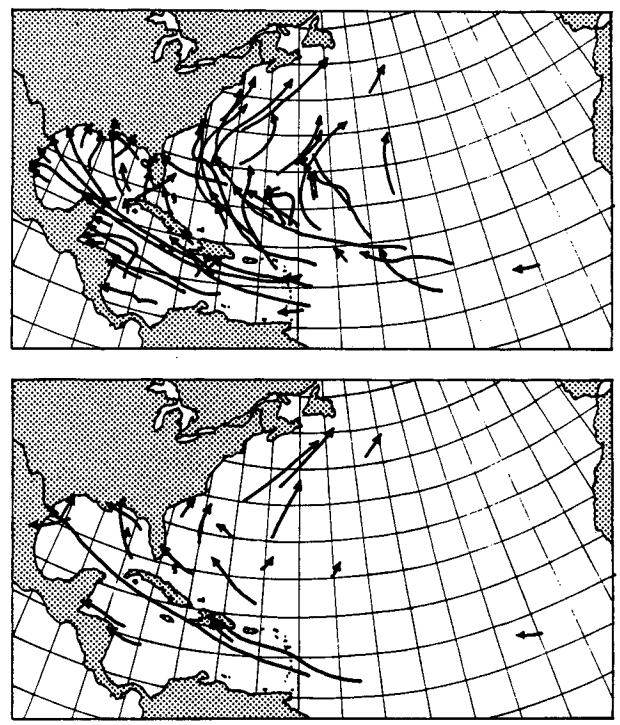

FIG. 3. Tracks of intense hurricanes during the 15 yr when the extrapolated QBO 50-mb zonal winds and the wind shear to 30 mb had the lowest values (top diagram) versus those 15 yr when this sum was the largest (bottom diagram) of the 41-yr period of 1950–1990.

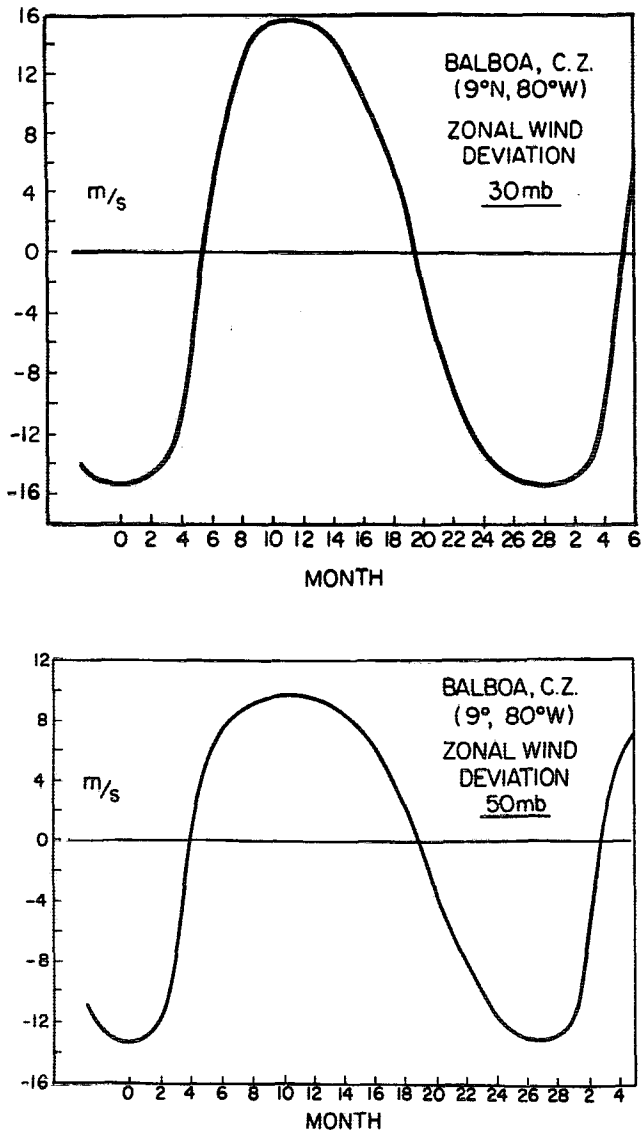

FIG. 4. Composite climatology of 30-mb and 50-mb relative zonal wind at Balboa (latitude 9°N) as determined from 1950 to 1987.

value of the stratospheric QBO winds at latitudes of 10°–15°N are strongly from the east. This condition causes net advection of hurricane structural elements that extend into the lower stratosphere away from the hurricane center. This relative advection is likely to act to restrain the stratospheric contribution to hurricane development and intensification. By contrast, during the west phase of the QBO, the absolute value of the zonal wind in the stratosphere (over hurricanes) at 10°–15°N is weak. In this case, comparatively small horizontal wind ventilation may occur in the lower stratosphere (Fig. 2). This west-phase condition is a positive influence on the inner-core intensity of developing hurricanes. In this way the QBO west phase is a positive cyclone influence, and the east phase a negative influence. Additionally, it is possible that the QBO exerts other dynamical influences upon the large-scale environment within which the hurricanes form. These involve hydrostatic height and temperature field differences associated with east and west phases of the QBO. Recent work (e.g., Gray et al. 1992a,b) shows support for these ideas; however, continued research into the QBO–tropical cyclone association is needed.

b. Methodology for forward extrapolation of QBO

The stratosphere QBO is special in that it may be the only atmospheric phenomena that can be extrapolated accurately ten months into the future. Although the QBO cycle is the most predictable of all long-term wind variations, it is still observed to have a 20%–30% variability in both period and amplitude. This variability inevitably leads to inaccuracies in 10-month forward extrapolations of the cycle. Two sources of error are possible in estimating the future trends in the QBO. For the purposes at hand, these include: 1) the proper location of the November QBO wind in relation to the current QBO wind cycle and 2) the possible departure of the (future) ten-month QBO trend from the changes expected based on the long-term climatology of 17 QBO cycles since 1950. These potential errors are recognized, and may not be too restrictive. We find that typically, skillful estimates of the future magnitude of the QBO zonal wind can be made ten months in advance.

Figure 4 shows the climatology of the Balboa, Canal Zone, (9°N) stratospheric QBO zonal-wind variability

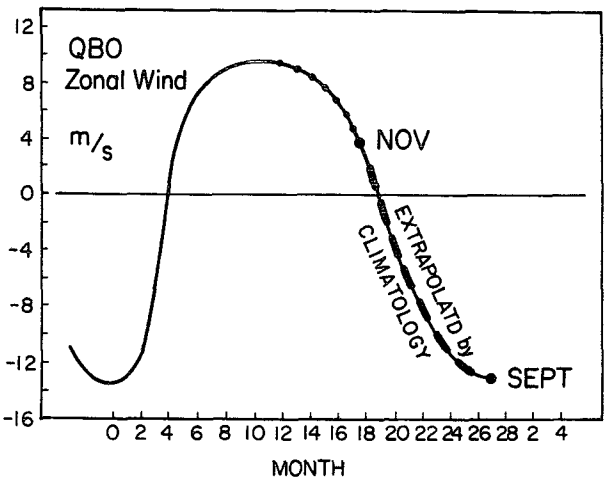

FIG. 5. Example of how the QBO relative zonal wind would be extrapolated from November–September from the climatology once the proper positioning of November wind has been made. Once the position of the November wind (in this case +4 m s^{-1}) within the relative cycle was determined, a climatologically specified ten-month extrapolation to September of the next year can be made.

(relative to the annual cycle) that occurs at 50 mb (~20-km altitude) and at 30 mb (~23 km). These curves were constructed by averaging the periods and magnitude of each QBO relative wind shift at Balboa for the 38 years of 1950–1987. This figure can be used to specify the location (phase) of the current (i.e., November) QBO wind in relation to the full cycle. Date positioning within the QBO cycle can usually be well estimated in relation to the date of the last zero crossing (i.e., west-to-east or east-to-west phase transition). Westerly and easterly periods at 30 mb typically last about 14.5 and 13.5 months, respectively, with a bias to longer westerly and shorter easterly periods at 50 mb.

The position of the November 30-mb and 50-mb zonal wind in relation to the phase of the QBO cycle is estimated by noting the number of months since the last reversal of sign. If, in November, 30-mb winds had switched from easterly to westerly anomalies nine months previously, then we would judge from climatology that the next westerly-to-easterly transition would occur six months later (by the next June). We

TABLE 3. Listing of months into westerly or easterly phase of each November period between 1950 and 1990 with next September year of application.

50 mb (20 km)				30 mb (23 km)			
Year of November determination	Months since first westerly	Months since first easterly	Year of September application	Year of November determination	Month since first westerly	Month since first easterly	Year of September application
1949*		6	→ 1950	1949*		8	→ 1950
1950	3		→ 1951	1950	4		→ 1951
1951	16		→ 1952	1951		3	→ 1952
1952		10	→ 1953	1952	5		→ 1953
1953	12		→ 1954	1953		1	→ 1954
1954		9	→ 1955	1954	1		→ 1955
1955	9		→ 1956	1955	13		→ 1956
1956		7	→ 1957	1956		8	→ 1957
1957	6		→ 1958	1957	8		→ 1958
1958		4	→ 1959	1958		7	→ 1959
1959	4		→ 1960	1959	6		→ 1960
1960		6	→ 1961	1960		8	→ 1961
1961	6		→ 1962	1961	11		→ 1962
1962		2	→ 1963	1962		8	→ 1963
1963	3		→ 1964	1963	5		→ 1964
1964	15		→ 1965	1964	16		→ 1965
1965		4	→ 1966	1965		12	→ 1966
1966	5		→ 1967	1966	7		→ 1967
1967	7		→ 1968	1967		5	→ 1968
1968		9	→ 1969	1968		16	→ 1969
1969	6		→ 1970	1969	9		→ 1970
1970		6	→ 1971	1970		11	→ 1971
1971	5		→ 1972	1971	10		→ 1972
1972		5	→ 1973	1972		7	→ 1973
1973	7		→ 1974	1973	11		→ 1974
1974		5	→ 1975	1974		11	→ 1975
1975	4		→ 1976	1975	6		→ 1976
1976		1	→ 1977	1976		4	→ 1977
1977		13	→ 1978	1977	3		→ 1978
1978	9		→ 1979	1978		0	→ 1979
1979		5	→ 1980	1979		10	→ 1980
1980	5		→ 1981	1980	9		→ 1981
1981		1	→ 1982	1981		7	→ 1982
1982	1		→ 1983	1982	4		→ 1983
1983	14		→ 1984	1983		5	→ 1984
1984		7	→ 1985	1984		16	→ 1985
1985	6		→ 1986	1985	12		→ 1986
1986		1	→ 1987	1986		6	→ 1987
1987	2		→ 1988	1987	4		→ 1988
1988	14		→ 1989	1988	16		→ 1989
1989		6	→ 1990	1989		10	→ 1990
1990	6		→ 1991	1990	9		→ 1991

* Data for 1949 was obtained by backward extrapolation.

would expect that by the following September the QBO would be three months into a new easterly phase of the QBO cycle. Figure 5 shows how this extrapolation would be made. Table 3 lists the duration in months of the westerly and easterly phases of the QBO at 50 mb and 30 mb prior to each November between 1950 and 1990.

Separate extrapolations are made for the 30-mb and 50-mb levels. Once these 10-month (or current November to next September) extrapolations of the QBO winds are made, corrections for the annual wind cycle at 10°N latitude are made for each level, and estimated values for the absolute zonal winds are obtained. We find that this simple quantitative extrapolation gives accurate and reproducible estimates of September QBO winds for the following year. This ten-month extrapolation is quite easy to apply, requiring only the number of months since the previous QBO phase transition, west to east, or vice versa. The expected climatologically specified ten-month extrapolated winds for the following September can then be read from Table 4.

The November QBO wind can also be used as an aid to adjust for longer-than-average QBO periods. For instance, the 30-mb QBO westerly wind mode is sometimes observed to persist for periods as long as 18 months. If November zonal winds are still westerly after 16 or 17 months or are still *strongly* westerly after 14 or 15 months, then this westerly cycle can be judged to be longer than normal. In this case, a 2–3-month backward time correction is appropriate for the November positioning within the westerly cycle. Note in Table 4 that provision is made to account for such extended period occurrences.

Values of 10-month climatologically extrapolated 30-mb and 50-mb September zonal winds for the period of 1950–1990 are given in Table 5; values for observed winds are shown in the second column. The actual winds minus the extrapolated winds, or the extrapolation error, are given in the last column. The mean of the error for these extrapolated winds is only about 40% as large as the mean error for the September wind estimates based only on the September climatological wind. Hence, we can definitely make improved estimates relative to mean conditions using this 10-month extrapolation procedure.

TABLE 4. September forecast QBO wind at 10°N latitude from previous November as a function of the number of months to November that change to westerly (left side) or easterly (right side) relative wind has occurred.

Months since change to westerly of November wind	10-month September forecast (m s^{-1})	Months since change to easterly of November wind	10-month September forecast (m s^{-1})
	50 mb (20 km)		
0	−1	0	−22
1	−2	1	−21
2	−3	2	−17
3	−4	3	−14
4	−6	4	−9
5	−8	5	−5
6	−12	6	−3
7	−14	7	−2
8	−17	8	−1
9	−19	9	0
10	−20	10	0
11	−22	11	−1
12	−23	12	−1
13	−23	13	−2
14	−23	14	−2
15	−23	15	−3
16	−23	16	−4
17	−23	17	−6
18	−23		
	30 mb (23 km)		
0	−3	0	−32
1	−4	1	−32
2	−5	2	−30
3	−9	3	−26
4	−13	4	−24
5	−18	5	−14
6	−21	6	−9
7	−25	7	−5
8	−28	8	−3
9	−30	9	−1
10	−31	10	−1
11	−32	11	−2
12	−32	12	−2
13	−32	13	−3
14	−32	14	−5
15	−32	15	−7
16	−32	16	−9
17	−32	17	−11
18	−32		

3. African rainfall as a long-range predictor of hurricane activity

a. Western Sahel rainfall

The Sahel is the transition zone between the Sahara Desert to the north and the rainforest region of the Guinea Coast. During the last few decades much of the Sahel has experienced large year-to-year persistent rainfall anomalies (Nicholson 1979). In general, wet years were followed by wet years (e.g., in the 1950s and 1960s), while dry years often follow dry years (e.g., in the 1970s and 1980s). This persistence provides a moderate amount of skill for the forecasting of Atlantic hurricane activity because of the strong concurrent association of western Sahel rain to Atlantic basin hurricanes (Gray 1990a; Landsea 1991; Landsea and Gray 1992; Landsea et al. 1992).

Utilizing data from 38 western Sahel rainfall stations (Fig. 6) that are described in Landsea and Gray (1992), a standardized index of western Sahel rainfall has been constructed during the two wettest months of August

TABLE 5. Comparison of November–September ten-month extrapolated (forecast) QBO zonal winds versus actual (observed) September winds. Positive forecast errors indicate an overestimation of the zonal winds; negative, an underestimate. (Values in m s^{-1}).

	50 mb (20 km)			30 mb (23 km)		
Year	Forecast September wind	Observed September wind	Forecast error	Forecast September wind	Observed September wind	Forecast error
1950	−3	−3	0	−3	−2	−1
1951	−4	−8	4	−13	−19	6
1952	−23	−19	−4	−26	−8	−18
1953	0	−5	5	−18	−13	−5
1954	−23	−23	0	−32	−25	−7
1955	0	0	0	−4	−4	0
1956	−19	−18	−1	−33	−29	−4
1957	−2	−2	0	−3	−10	7
1958	−12	−14	2	−28	−30	2
1959	−9	0	−9	−5	1	−6
1960	−6	−15	9	−21	−26	5
1961	−3	−2	−1	−3	−4	1
1962	−12	−10	−2	−32	−27	−5
1963	−17	−8	−9	−3	−8	5
1964	−4	1	−5	−18	−11	−7
1965	−23	−16	−7	−32	−31	−1
1966	−9	−4	−5	−2	−2	0
1967	−8	−6	−2	−25	−17	−8
1968	−23	−20	−3	−14	−31	17
1969	0	−3	3	−9	−6	−3
1970	−12	−21	9	−30	−31	1
1971	−3	−3	0	−2	−10	8
1972	−8	−19	11	−31	−28	−3
1973	−5	−4	−1	−5	−10	5
1974	−14	−18	4	−32	−31	−1
1975	−5	−5	0	−2	−3	1
1976	−6	−7	1	−21	−21	0
1977	−21	−23	2	−24	−11	−13
1978	−2	−1	−1	−9	−12	3
1979	−19	−17	−2	−31	−29	−2
1980	−5	−2	−3	−1	−2	1
1981	−8	−8	0	−30	−26	−4
1982	−21	−15	−6	−5	−1	−4
1983	−2	−6	4	−13	−23	10
1984	−23	−26	3	−14	−32	18
1985	−2	1	−3	−9	−3	−6
1986	−12	−8	−4	−32	−23	−9
1987	−21	−14	−7	−9	3	−12
1988	−3	−4	1	−13	−17	4
1989	−23	−18	−5	−32	−29	−3
1990	−3	−6	2	−1	−6	5

and September. This index is made of the average of the standardized deviation of each station. Note how most of the years of the 1950s and 1960s were wet, while those of the 1970s and 1980s were dry. Yearly values of this index are shown in Fig. 7 and listed in Table 1.

Figure 7 shows the strong multidecadal rainfall variations that have affected the western Sahel since the late 1960s. Such multidecadal controls on West African rainfall are likely linked to long-term (interdecadal) sea surface temperature anomaly patterns around the globe (Folland et al. 1986). It is also possible that the persistence of low rainfall (especially during the drought-stricken 1970s and 1980s) has contributed to natural changes of the land surface (Nicholson 1988) and to related anthropogenic alterations in the land surface, such as overgrazing and deforestation (Charney 1975). Either of these effects may contribute to alterations of the West African monsoonal circulation, and, hence, of the embedded squall lines, as a result of differences in surface moisture availability and land-surface temperature.

Table 6 gives statistical information on the hurricane activity during seasons one year after each of the ten wettest and each of the ten driest western Sahel August and September periods between 1949 and 1989. Note

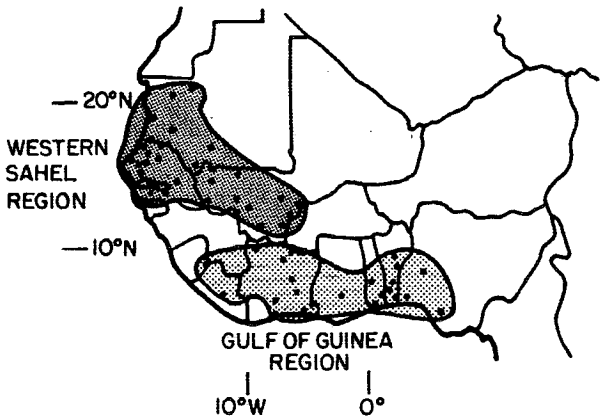

FIG. 6. Locations of rainfall stations that make up the 38-station August–September western Sahel precipitation index and the 24-station August–November Gulf of Guinea precipitation index.

the modulation of the hurricane activity wherein there is only a modest difference in the total number of hurricanes, but a nearly two to one (wet/dry) difference for the seasonal incidence of intense hurricane days. Figure 8 portrays differences in the intense-(category 3-4-5) hurricane tracks for these two ten-year rainfall classes. Note the many more intense-hurricane tracks in the Atlantic in the area to the east of Florida during wet rather than dry years.

b. *Gulf of Guinea rainfall*

Landsea (1991) has documented a surprisingly strong predictive signal for seasonal intense Atlantic hurricane activity based on August–November rainfall along the Gulf of Guinea of the previous year. As with the Sahel rainfall data, rainfall from 24 Gulf of Guinea locations (shown in Fig. 6) is combined in terms of the mean standardized deviation for the region. Figure 9 presents the yearly variations in this rainfall index for 1949–1990.

TABLE 6. Comparison of average hurricane activity in the hurricane seasons a year after each of the ten wettest western Sahel (Fig. 6) August–September periods versus the ten seasons a year after each of the ten driest periods between 1949 and 1989.

	Ten wettest	Ten driest	Ratio
No. of hurricanes	6.2	5.8	1.07
No. of hurricane days	26.8	19.3	1.39
No. of intense hurricanes	3.1	2.0	1.55
No. of intense-hurricane days	7.2	3.6	1.99

The variations in seasonal hurricane activity 6–11 months after each of the ten wettest and each of the ten driest August–November periods in the Gulf of Guinea rainfall are shown in Table 7. This extended-range association appears to be the strongest of any of the individual predictors. Note that in the ten hurricane seasons following the ten wettest Gulf of Guinea periods, the rate of intense-hurricane days activity was four times the level of that which occurred during the

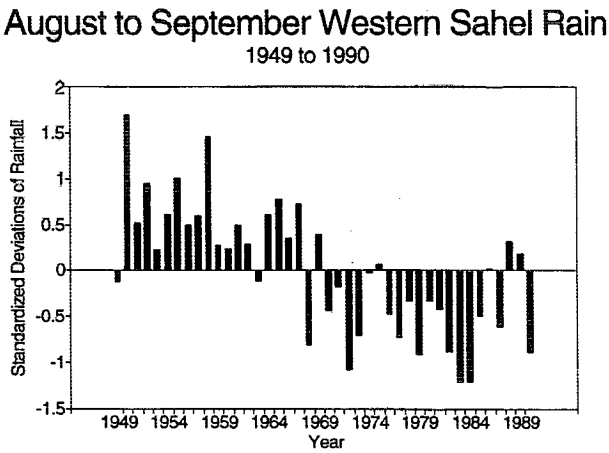

FIG. 7. Mean standardized deviations of rainfall for the 38-station August–September western Sahel rainfall index. Data are analyzed for the years 1949–1990.

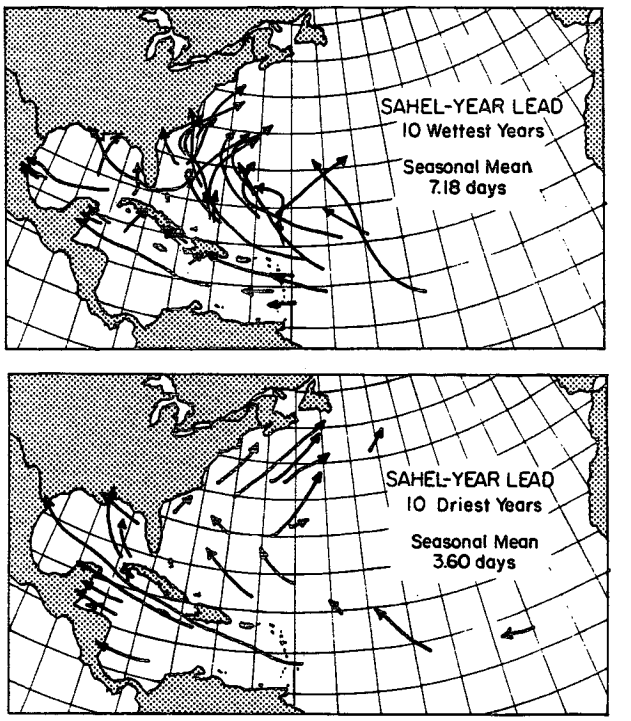

FIG. 8. Tracks of intense hurricanes in the years following the ten wettest (top diagram) August–September western Sahel years versus the ten driest periods (bottom diagram) for the years 1949–1989.

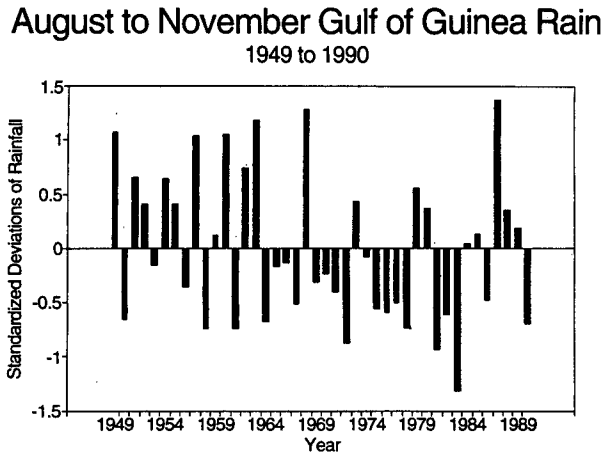

FIG. 9. Mean standardized deviations of rainfall for the 24-station August–November Gulf of Guinea rainfall index. Data presented are from 1949 to 1990.

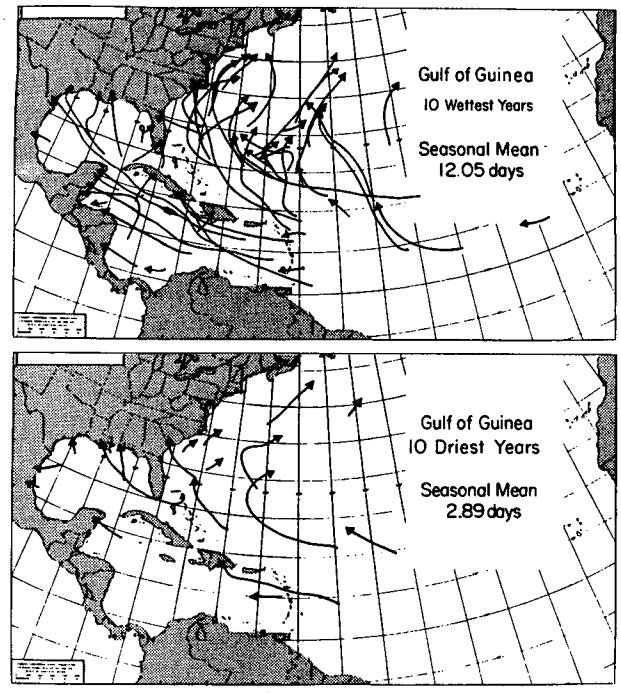

FIG. 10. Tracks of intense hurricanes in the years following the ten wettest (top diagram) August–November Gulf of Guinea years versus the ten driest periods (bottom diagram) for the years 1949–1989.

hurricane seasons following the ten driest Gulf of Guinea periods, and the number of intense hurricanes was 2.6 times as many. This difference is also reflected in Fig. 10, where the composited tracks of individual intense hurricanes are shown for both the ten wettest and the ten driest Gulf of Guinea seasonal periods. Landsea (1991) has shown that the strong correlations between these rainfall data and the seasonal hurricane data are unaffected by a linear detrending of both datasets.

The strong association realized between the Atlantic basin hurricane activity and prior-year Gulf of Guinea rainfall is likely due to feedbacks on the monsoon circulation from one year to the next. As discussed by Landsea (1991), heavy rainfall along the Gulf of Guinea as the summer monsoon retreats southward from August to November may provide an enhanced moisture source that contributes to a strong onset of the next year's monsoon. This moisture may be available through soil moisture and evapotranspiration from the biosphere. Thus, abundant rainfall along the Gulf of Guinea may lead to more rain in the Sahel during the following year and greater Atlantic basin hurricane activity. Conversely, a drier August to November period along the Gulf of Guinea may contribute to drought in the Sahel several months later. Such droughts are typically associated with much reduced intense-hurricane activity (Fig. 10).

In the following section we perform independent statistical tests on stratospheric QBO and West African rainfall data for the 41-yr period from 1949 through 1989 to determine the extent (skill level) to which the QBO and West African rainfall data can be used for long-range (ten-month lead time) seasonal hurricane forecasts.

TABLE 7. Comparison of average hurricane activity in the seasons following the ten wettest August to November periods along the Gulf of Guinea versus the ten driest periods for the years 1949–1989.

	Ten wettest	Ten driest	Ratio
No. of hurricanes	8.0	4.6	1.74
No. of hurricane days	39.0	17.7	2.20
No. of intense hurricanes	4.7	1.8	2.61
No. of intense-hurricane days	12.0	2.9	4.16

4. Analyses and results

The statistical methodology for the analysis of the data consists of four distinct, but interrelated, steps:

1) Least-absolute deviation regression provides prediction values, based on a forecast model, for each of the $n = 41$ yr. In the construction of any forecast model, it is imperative that the model be developed on a subset of the data and then independently tested on a different subset of the data that was not used in the formulation of the model. This cross validation of a forecast model may be accomplished by means of a jackknife procedure.

2) A cross-validation (jackknife) procedure ensures that the prediction for any year is independent of the

TABLE 8. Empirical weights for composite functions of wind and rainfall from a jackknife solution.

	Wind			Rainfall	
	a_1	a_2	a_3	a_4	a_5
Named storms	1.000	0.252	−0.640	1.000	2.498
Named storm days	1.000	0.424	−0.316	1.000	2.390
Hurricanes	1.000	−0.320	−3.384	1.000	2.302
Hurricane days	1.000	1.781	−1.370	1.000	2.144
Intense hurricanes	1.000	0.103	−1.415	1.000	2.455
Intense-hurricane days	1.000	−0.080	−1.410	1.000	2.292
Hurricane destruction potential	1.000	1.066	−1.346	1.000	1.700

observations for that year. Since the purpose of the present methodology is to forecast a single year, $n - 1 = 41 - 1 = 40$ yr of data are used for the formulation of each forecast model, and each model is then tested on the remaining 1 yr of independent data not used in the construction of the model. This procedure is repeated 41 times, yielding 41 prediction values for each of 7 seasonal dependent variables.

3) The cross-validated prediction values and the observed values for each of the $n = 41$ yr are compared by calculating a measure of agreement.

4) The probability of the measure of agreement is obtained under the null hypothesis. Details of this statistical methodology are presented in appendix B.

The prediction equation for each of the seasonal dependent variables (i.e., named storms, named storm days, hurricanes, hurricane days, intense hurricanes, intense-hurricane days, and hurricane destruction potential) is

$$\hat{y} = \hat{\beta}_0 + \hat{\beta}_1 W + \hat{\beta}_2 R, \quad (1)$$

where $\hat{y}$ represents one of the seven dependent variables, $\hat{\beta}_0$, $\hat{\beta}_1$, and $\hat{\beta}_2$ are the LAD regression weights determined from a nonjackknife solution (see appendix B), W is a composite function of the extrapolated (November to September) upper-air zonal winds at 50 mb (U_{50}) and 30 mb (U_{30}), where

$$W = a_1 U_{50} + a_2 U_{30} + a_3 |U_{50} - U_{30}|, \quad (2)$$

TABLE 9. Agreement coefficient (ρ), probability (P), and r^2 values from a jackknife solution.

	ρ	P	r^2
Named storms	0.440	0.22×10^{-5}	0.395
Named storm days	0.514	0.89×10^{-7}	0.488
Hurricanes	0.447	0.15×10^{-5}	0.466
Hurricane days	0.491	0.46×10^{-6}	0.511
Intense hurricanes	0.498	0.95×10^{-7}	0.581
Intense-hurricane days	0.451	0.27×10^{-6}	0.517
Hurricane destruction potential	0.447	0.11×10^{-5}	0.527

TABLE 10. Regression weights from a nonjackknife solution for prediction equations.

	$\hat{\beta}_0$	$\hat{\beta}_1$	$\hat{\beta}_2$
Named storms	11.732	0.135	0.701
Named storm days	64.072	1.031	7.149
Hurricanes	7.560	0.049	0.759
Hurricane days	33.303	0.215	6.645
Intense hurricanes	3.571	0.042	0.717
Intense-hurricane days	7.605	0.124	2.006
Hurricane destruction potential	95.326	0.686	24.747

and R is a composite function of August–September western Sahel (R_S) and August–November Gulf of Guinea (R_G) rainfall, where

$$R = a_4 R_S + a_5 R_G. \quad (3)$$

The weights (a_1, a_2, a_3, a_4, and a_5) for each of the predictor variables are given in Table 8 for each of the dependent variables. These weights were empirically determined, with LAD regression and the jackknife solution, to maximize the agreement coefficient (ρ) described in appendix B.

The agreement coefficients (ρ) and their associated probability values (P) are given in Table 9. For comparative purposes only, the corresponding values of the squared Pearson cross-product correlation coefficient (r^2) are presented in the last column of Table 9. Since the results of Table 9 are based on the cross-validated LAD criterion, the values of r^2 are not maximized. While r^2 is strictly a measure of linearity (i.e., $r^2 = 1$ implies all observed and predicted value pairs fall on a line that does not necessarily have a unit slope or pass through the origin), ρ is a measure of agreement, and $\rho = 1$ implies all observed and predicted value pairs fall on a line with unit slope that passes through the origin. Thus, the values of r^2 are often larger than the corresponding values of ρ; since r^2 depends on squared Euclidean distance residual values, r^2 can be smaller than ρ (Mielke 1984). The fact remains that r^2 is not a satisfactory measure of agreement. (Incidentally, had the jackknifed predictors been replaced with the nonjackknifed predictors, then all values of ρ and r^2 in Table 9 would have been larger. These larger values of ρ and r^2 are inappropriate, however, since independent validations of the predictions are necessary.)

In order to predict future results, regression weights ($\hat{\beta}_0$, $\hat{\beta}_1$, and $\hat{\beta}_2$) are required. Using 1) the jackknife solution weights for the predictor variables (a_1, a_2, a_3, a_4, and a_5), 2) LAD regression, and 3) a nonjackknife solution, the regression weights were calculated. Table 10 gives the regression coefficients for each dependent variable for future predictions. (Because the values of ρ and r^2 given in Table 9 are based on cross-validated LAD predictors, they will be smaller than the

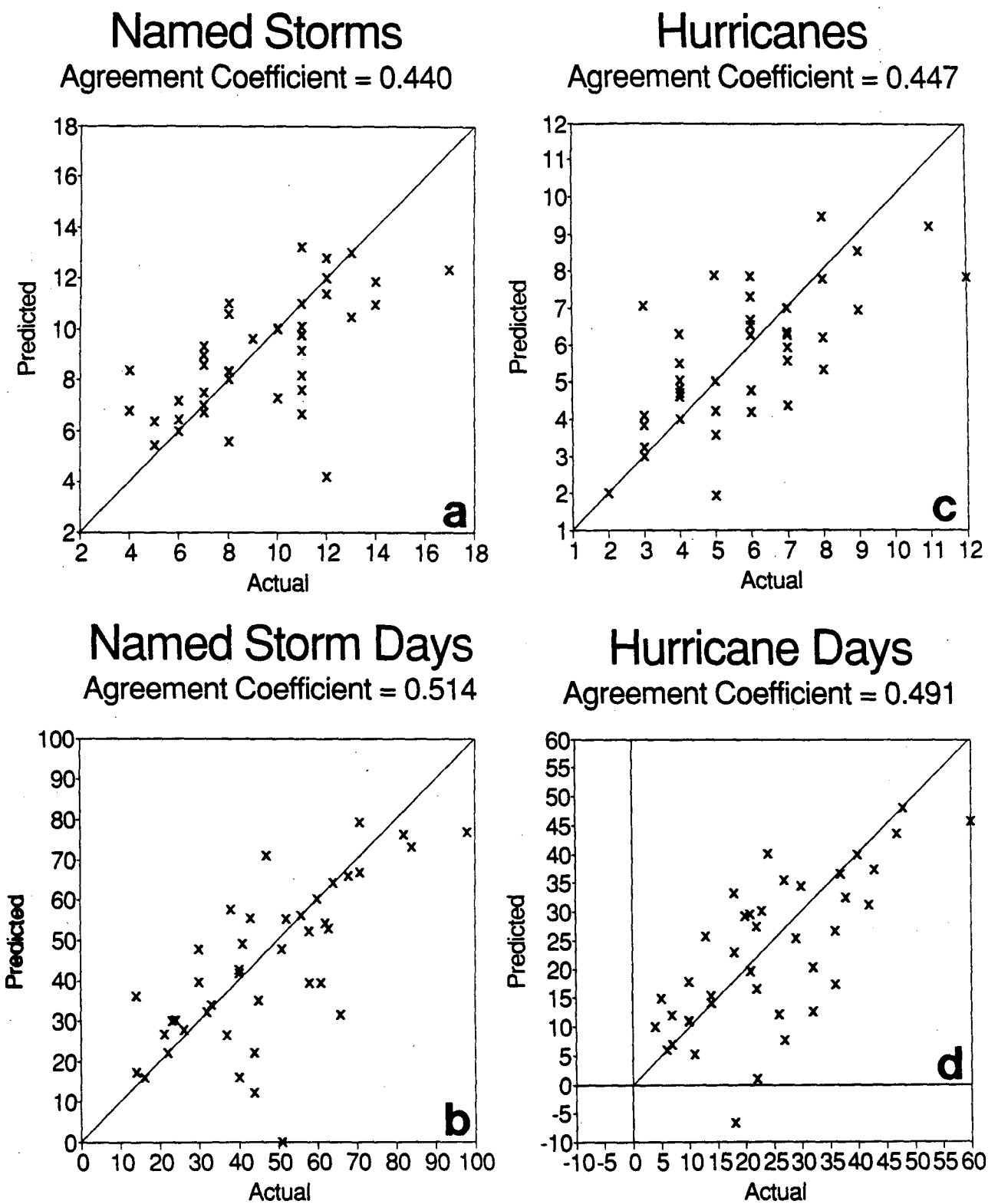

FIG. 11. Scatter plots of predicted jackknife versus actual observed seasonal number of (a) named storms, (b) named storm days, (c) hurricanes, (d) hurricane days, (e) intense hurricanes, (f) intense-hurricane days, and (g) hurricane destruction potential (HDP) for hindcast between 1950 and 1990.

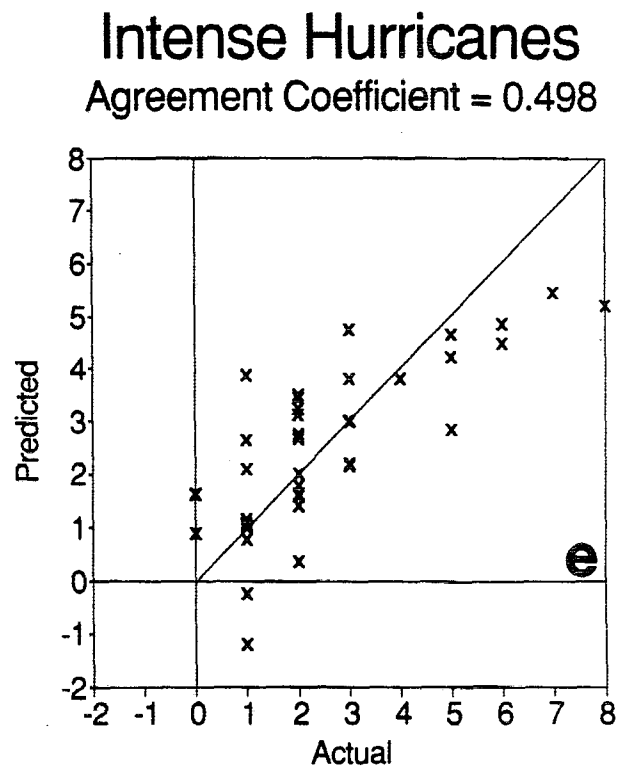

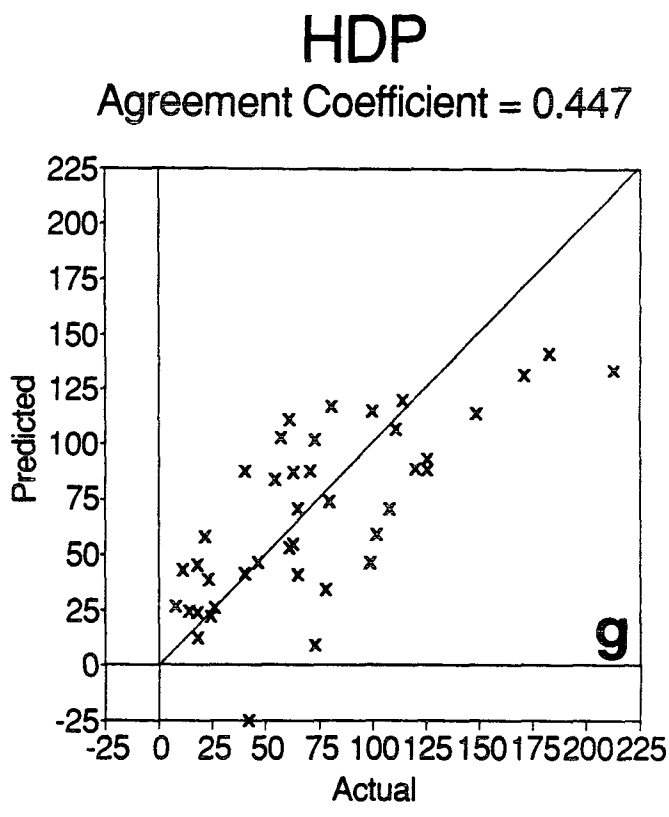

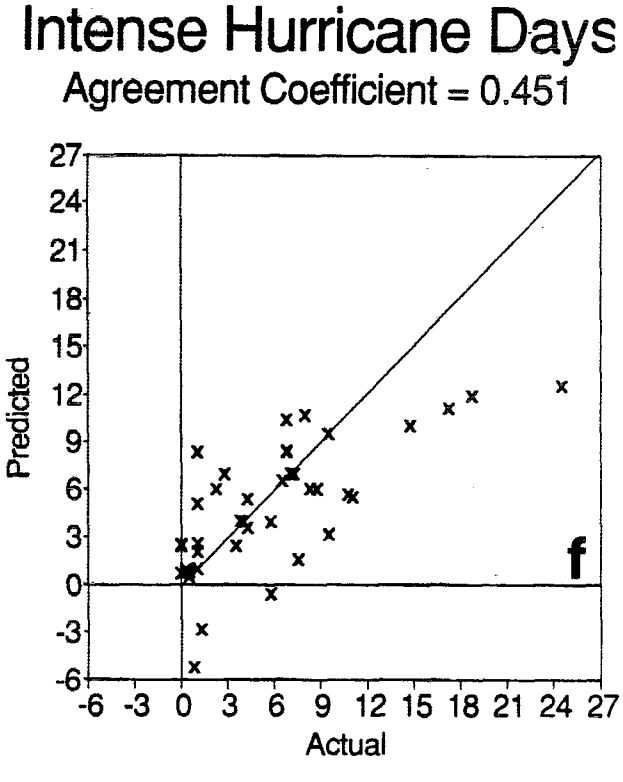

FIG. 11. (*continued*)

corresponding values of ρ and r^2 based on the non-jackknife regression coefficients in Table 10.) Substituting (2) and (3) into (1) yields the prediction equation given by

$$\hat{y} = \hat{\beta}_0 + \hat{\beta}_1(a_1U_{50} + a_2U_{30} + a_3|U_{50} - U_{30}|) + \hat{\beta}_2(a_4R_S + a_5R_G). \quad (4)$$

As an example of the seasonal forecasts, the coefficients of Tables 8 and 10 yield the following prediction equation for the seasonal number of intense hurricanes (IH):

$$\text{IH} = 3.571 + 0.042 \times (1.0U_{50} + 0.103U_{30} - 1.415|U_{50} - U_{30}|) + 0.717(1.0R_S + 2.455R_G). \quad (5)$$

The diagrams of Fig. 11 present the scatter plots of the predicted values of each of the seven predictors versus the observed values. While the dependence between predicted and observed values is visually apparent, this empirical model is obviously imperfect. When a prediction is negative, as observed for HD, IH, IHD, and HDP, a zero should, of course, replace a predicted negative value. A further feature specifically involving IH, IHD, and HDP is that the models tend to underestimate observed values that are extremely large. Awareness of this underestimation bias and the negative forecasts allows one to subjectively alter the cases in question, and a somewhat higher forecast skill may be obtained.

Note in Table 9 that we can independently (jackknife) hindcast over 44% of the measure of agreement value (ρ) for all seven forecast parameters. In fact, we can hindcast over 49% of the value of ρ for the seasonal number of named storm days, number of intense hurricanes, and number of intense-hurricane days. The probability that there is no hindcast statistical skill in any of these forecast parameters is between 10^{-5} and 10^{-8}.

5. Discussion

It is remarkable that Atlantic seasonal hurricane activity, manifesting itself as sporadic mesoscale events, would show such a strong association with forcing functions so far removed in space and time. This association is further evidence for the primary role of global and regional circulation patterns in governing seasonal hurricane frequency and intensity. Recent research by Gray (1988) and others further illustrates the fundamental role of the large-scale and global circulation patterns in determining the frequency and the intensity with which the smaller-scale mesoscale weather events are able to develop into hurricanes. Previously, we had viewed hurricanes, along with the weaker weather systems that spawned them, as the product of rapidly varying local circulation characteristics that had a large random component and that were impossible to predict a few days in advance, let alone ten months in advance. Although this view is still true for individual hurricane systems, it does not hold for the seasonal aggregate of hurricane systems. The climate signal has a strong influence in determining the number of short-lived and transitory events (i.e., hurricanes) that may be activated.

It was not expected that such strong relationships between climate and hurricanes would exist and have such long-period lag responses. If, in the future, the atmosphere continues to behave as it has over the last 41 yr, then a considerable amount of extended-range future seasonal forecast skill is available. We have no reason for thinking that the atmosphere will not continue to behave during the next few decades as it has during the last four decades. Forecast skill during the first 20-yr period differed little from the last 21-yr period.

Skillful extended-range prediction, at least of Atlantic seasonal hurricane activity, is indeed possible. Considering the difficulties inherent in any seasonal weather-prediction scheme plus the extraordinary 6–11-month extended range of this relationship, we consider this to be an important finding. Until recently, few serious researchers would have imagined that there might be seasonal predictive signals this strong extending this far into the future. In addition, full exploitation of all potential Atlantic predictive signals has not yet been made. Further study of additional unexploited regional or global variables, including West African land temperatures, land and ocean surface pressure, Atlantic SSTs, plus other potential seasonal predictors, have not yet been accomplished. Consequently, it is most likely that further improvements are possible with additional research.

Acknowledgments. The authors wish to thank Richard Taft and William Thorson for their very expert assistance in the processing of the West African rainfall data and to John D. Sheaffer for many beneficial discussions and for assistance in manuscript preparation.

We are very grateful for the West African rainfall data supplied to us by William Spangler and Roy Jenne of the National Center for Atmospheric Research (NCAR). Much of the data came from the extensive African rainfall collections originally compiled by Sharon Nicholson of Florida State University, Graham Farmer of the US AID/Fews Project, Peter Lamb of the University of Oklahoma, Douglas Le Comte of the US AID program, Dave Miskus and R. J. Tinker of the NOAA Climate Analysis Center, and E. O. Oladipo of Ahmodu Bello University of Nigeria. James Angell provided QBO wind information. Barbara Brumit and Laneigh Walters provided expert assistance in manuscript preparation and data analysis.

This research was supported primarily by a climate grant from the National Science Foundation, with

supplemented assistance from the NOAA Office of Global Programs.

APPENDIX A

Definitions

Atlantic basin. The area including the entire Atlantic Ocean, the Caribbean Sea, and the Gulf of Mexico.
Tropical cyclone (TC). A large-scale circular flow occurring within the tropics and subtropics that has its strongest winds at low levels, including hurricanes, tropical storms, and other weaker rotating vortices.
Tropical storm. A tropical cyclone with maximum sustained winds between 39 (18 m s^{-1} or 34 kt) and 73 (32 m s^{-1} or 63 kt) miles per hour.
Named storm (NS). A hurricane or a tropical storm.
Named storm day (NSD). Four 6-h periods during which a tropical cyclone is observed or estimated to have attained tropical-storm or hurricane-intensity winds.
Hurricane (H). A tropical cyclone with sustained low-level winds of 74 miles per hour (33 m s^{-1} or 64 kt) or greater.
Hurricane day (HD). Four 6-h periods during which a tropical cyclone is observed or estimated to have hurricane-intensity winds.
Intense hurricane (IH). A hurricane reaching at some point in its lifetime a sustained low-level wind of at least 111 mph (96 kt or 50 m s^{-1}). This constitutes a category 3 or higher on the Saffir–Simpson scale (Simpson 1974).
Intense-hurricane day (IHD). Four 6-h periods during which a hurricane has intensity of Saffir–Simpson category 3 or higher.
Hurricane destruction potential (HDP). A measure of a hurricane's potential for wind and storm-surge destruction defined as the sum of the square of a hurricane's maximum wind speed for each 6-h period of its existence. Values are given in 0.25×10^4 $(m\ s^{-1})^2$.
Saffir–Simpson (S–S) *category.* A measurement scale (1–5) of a hurricane's wind and ocean-surge intensity. One is the weakest hurricane, 5 the most intense hurricane (Simpson 1974).

APPENDIX B

Statistical Methodology

The statistical methodology for the analysis of the data consists of four distinct, but interrelated, steps: 1) Least-absolute deviation regression provides prediction values for each of the n years. 2) A cross-validation (jackknife) procedure ensures that the prediction for any year is independent of the observations for that year. 3) The cross-validated predicted values and observed values for all n years are compared by calculating a measure of agreement. 4) The probability that the observed measure of agreement occurred by chance alone (the null hypothesis) is obtained.

Ordinary least-squares (OLS) regression analysis yields efficient and unbiased estimates of population regression parameters and their associated standard errors when the population is Gaussian (or multivariate Gaussian) with equal variances (or a variance–covariance matrix that exhibits compound symmetry). The OLS is far from optimal in many non-Gaussian situations, especially when the population distribution is asymmetric and/or when outlying values are present. Even a modest departure from a Gaussian distribution can seriously degrade the efficiency of OLS estimates (Kowalski 1972; Rey 1983; Micceri 1989). The problems generated by non-Gaussian distributions and/or extreme values are common in weather and forecast data. One of the most satisfying robust alternatives to OLS regression is least-absolute deviation (LAD) regression (Barrodale and Roberts 1973, 1974; Bloomfield and Steiger 1980; Dielman 1984; Gentle et al. 1977; Mielke 1987; Narula and Wellington 1982; Seneta 1983). The LAD regression, which predates OLS regression (Sheynin 1973), is analogous to the use of the median in a univariate analysis to estimate the location of a distribution, since the median minimizes the sum of the absolute values of the residuals. For this reason, LAD regression estimates are 1) far more efficient than OLS estimates whenever the median is a better estimator of location than the mean and are 2) exceedingly more resistant than OLS regression to extreme values. As documented elsewhere (Mielke 1991; Sheynin 1973), C. F. Gauss (circa 1809) was unable to obtain the numerical solutions needed for LAD regression, and had to develop OLS regression as a default procedure. (Even though Gauss developed linear programming to implement LAD regression, the lack of any computational support made him realize that a simple calculus solution could implement OLS regression.)

To evaluate the prediction values of LAD regression, a cross-validation procedure is required. For any given year, the LAD prediction values are calculated from all remaining years when the dependent and independent observations of the given year are removed. This procedure is repeated for each of the n distinct years in question, and ultimately provides n independently predicted values.

The n observed values and the n corresponding predicted values are compared to see if they agree (i.e., are identical). The measure of agreement utilized in the analysis is a chance-corrected measure based on absolute differences between the n pairs of observed and predicted values (Berry and Mielke 1988; Mielke 1984, 1991).

Finally, the statistical significance of the agreement measure is determined. The observed measure of agreement value is compared against all possible values of the measure by obtaining the probability of having a value as large or larger than the observed measure of agreement under the null hypothesis.

For simplicity, let y_i denote the dependent variable and let $x_{i1}, \ldots, x_{ir}$ denote r independent variables associated with the ith of n events. Let $\tilde{y}_i$ denote the predicted value of y_i based on the r independent variables. In addition, $\tilde{y}_i$ is termed the cross-validated predictor of y_i since $\tilde{y}_i$ is determined only from the $n-1$ remaining events when the ith event is removed. Each $\tilde{y}_i$ is calculated from its associated LAD regression, where

$$\tilde{y}_i = \tilde{\beta}_{0i} + \sum_{j=1}^{r} \tilde{\beta}_{ji} x_{ij}$$

for $i = 1, \ldots, n$ and $(\tilde{\beta}_{0i}, \tilde{\beta}_{1i}, \ldots, \tilde{\beta}_{ri})$ are those values of $(\beta_0, \beta_1, \ldots, \beta_r)$ that minimize the sum of $n-1$ absolute differences given by

$$\sum_{i'(\neq i)} | y_{i'} - \beta_0 - \sum_{j=1}^{r} \beta_j x_{i'j} |$$

($\sum_{i'(\neq i)}$ denotes the sum of all events except the ith event). Furthermore, the nonjackknifed predictor of *y for future events* is given by

$$\hat{y} = \hat{\beta}_0 + \sum_{j=1}^{r} \hat{\beta}_j x_j,$$

where $(\hat{\beta}_0, \hat{\beta}_1, \ldots, \hat{\beta}_r)$ are those values of $\beta_0, \beta_1, \ldots, \beta_r$ that minimize the sum of n absolute differences given by

$$\sum_{i=1}^{n} | y_i - \beta_0 - \sum_{j=1}^{r} \beta_j x_{ij} |,$$

that is, the nonjackknifed predictor of y ($\hat{y}$) depends on all n events. The choice of LAD regression instead of OLS regression is that LAD regression is geometrically consistent with the data in question (Mielke 1985, 1986, 1987, 1991). The linear programming algorithm used to obtain the LAD regression estimates is due to Barrodale and Roberts (1973, 1974). The permutation procedure used to evaluate each regression is based on the statistic given by

$$\delta = \frac{1}{n} \sum_{i=1}^{n} | y_i - \tilde{y}_i |.$$

Thus, δ is the dispersion between y_i and $\tilde{y}_i$ (the jackknifed predictor of y_i) averaged over the n events. The observed value of δ (denoted by δ_0) is compared with the $n!$ possible values of δ where all $n!$ orderings of $\tilde{y}_1, \ldots, \tilde{y}_n$ are associated with the observed sequence $y_1, \ldots, y_n$. The null hypothesis dictates that all $n!$ possible values of δ are equally likely. Under the null hypothesis, the significance of δ_0 is given by

$$P\text{-value} = (\text{number of } \delta\text{'s} \leq \delta_0)/n!.$$

The accuracy of the n jackknifed predicted values $(\tilde{y}_1, \ldots, \tilde{y}_n)$, where each jackknifed prediction depends on the $n-1$ independent events using the previously described cross-validation procedure, requires a comparison with the n corresponding observed values $(y_1, \ldots, y_n)$. A measure of agreement between the corresponding y_i and $\tilde{y}_i$ values based on δ is given by

$$\rho = 1 - \delta/\mu_\delta,$$

where μ_δ is the expected value of δ under the null hypothesis. If $\rho = 1$, then perfect agreement is achieved (note that $\delta = 0$ implies that $y_i = \tilde{y}_i$ for $i = 1, \ldots, n$), whereas $\rho \leq 0$ implies no agreement. The process is continued until the cross-validation procedure's LAD estimates maximize the measure of agreement. Algorithms, computer programs, and discussion involving the P value and ρ are given elsewhere (Berry and Mielke 1988; Iyer et al. 1983; Mielke 1984, 1991; Mielke and Iyer 1982). A closely related alternative criterion to maximizing ρ is minimizing δ. The difference between these two criteria is that maximizing ρ is a nonlinear criterion (μ_δ depends on the regression coefficients), whereas minimizing δ is a linear criterion.

REFERENCES

Barrodale, I., and F. D. K. Roberts, 1973: An improved algorithm for discrete L_1 linear approximation. *S.I.A.M. J. Numer. Anal.*, **10,** 839–848.

——, and ——, 1974: Solution of an overdetermined system of equations in the L_1 norm. *Commun. Assoc. Comp. Mach.*, **17,** 319–320.

Berry, K. J., and P. W. Mielke, 1988: A generalization of Cohen's kappa agreement measure to interval measure and multiple raters. *Educ. Psych. Meas.*, **48,** 921–933.

Bloomfield, P., and W. Steiger, 1980: Least absolute deviations curve fitting. *Sci. Statist. Comput.*, **1,** 290–301.

Chan, J. C. L., 1991: Prediction of seasonal tropical cyclone activity over the western North pacific. Preprints, *Fifth Conf. on Climate Variations,* Denver, Amer. Meteor. Soc., 521–524.

Charney, J. G., 1975: Dynamics of desert and drought in the Sahel. *Quart. J. Roy. Meteor. Soc.*, **101,** 193–202.

Dielman, T. E., 1984: Least absolute value estimation in regression models: An annotated bibliography. *Commun. Stat.*, **A13,** 513–541.

Folland, C. K., T. N. Palmer, and D. E. Parker, 1986: Sahel rainfall and worldwide sea temperatures, 1901–85. *Nature,* **320,** 602–607.

Gentle, J. E., W. J. Kennedy, and V. A. Sposito, 1977: On least absolute deviations estimations. *Commun. Statist.*, **A6,** 839–845.

Gray, W. M., 1984a: Atlantic seasonal hurricane frequency. Part I: El Niño and 30 mb quasi-biennial oscillation influences. *Mon. Wea. Rev.*, **112,** 1649–1668.

——, 1984b: Atlantic seasonal hurricane frequency. Part II: Forecasting its variability. *Mon. Wea. Rev.*, **112,** 1669–1683.

——, 1985: Tropical cyclone global climatology. WMO Tech. Document WMO/TD-No. 72, Vol. I, WMO, Geneva, Switzerland, 3–19.

——, 1988: Environmental influences on tropical cyclones. *Aust. Meteor. Mag.*, **33,** 127–139.

——, 1990a: Strong association between west African rainfall and U.S. landfalling intense hurricanes. *Science,* **249,** 1251–1256.

——, 1990b: Summary of 1990 Atlantic tropical cyclone activity and seasonal forecast verification. Colorado State University, Department of Atmospheric Science. Fort Collins, CO, 29 pp.

——, J. D. Sheaffer, and J. A. Knaff, 1992a: A mechanism for the

modulation of ENSO variability by the stratospheric QBO. *J. Meteor. Soc. Japan,*

——, ——, and ——, 1992b: Hypothesized mechanism for stratospheric QBO influence on ENSO variability. *Geophys. Res. Lett.,* **19,** 107–110.

Iyer, H. K., K. J. Berry, and P. W. Mielke, 1983: Computation of finite population parameters and approximate probability values for multi-response randomized block permutation procedures (MRBP). *Commun. Stat.,* **B12,** 479–499.

Kowalski, C. J., 1972: On the effects of non-normality on the distribution of the sample product-moment correlation coefficient. *Appl. Stat.,* **21,** 1–12.

Landsea, C. W., 1991: West African monsoonal rainfall and intense hurricane associations. Department of Atmospheric Science. Paper No. 484, Colorado State University, Ft. Collins, CO, 272 pp.

——, and W. M. Gray, 1992: The strong association between western Sahel monsoon rainfall and intense Atlantic hurricanes. *J. Climate,* **5,** 435–453.

——, ——, P. W. Mielke, and K. J. Berry, 1992: Long-term variations of western Sahel monsoon rainfall and intense U.S. landfalling hurricanes. *J. Climate,* **5,** (in press).

Livezey, R. E., 1990: Variability of skill of long-range forecasts and implications for their use and value. *Bull. Amer. Meteor. Soc.,* **71,** 300–309.

Micceri, T., 1989: The unicorn, the normal curve, and other improbable creatures. *Psych. Bull.,* **105,** 156–166.

Mielke, P. W., 1984: Meteorological applications of permutation techniques based on distance functions. *Handbook of Statistics, Vol. 4: Nonparametric Methods,* P. R. Krishnaiah and P. K. Sen, Eds., North-Holland Publishing Co., 813–830.

——, 1985: Geometric concerns pertaining to statistical tests in the atmospheric sciences. *J. Atmos. Sci.,* **42,** 1209–1212.

——, 1986: Non-metric statistical analyses: Some metric alternatives. *J. Stat. Plann. Inference,* **13,** 377–387.

——, 1987: L_1, L_2 and L_∞ regression models: Is there a difference? *J. Stat. Plann. Inference,* **16,** 430.

——, 1991: The application of multivariate permutation methods based on distance functions in the earth sciences. *Earth-Sci. Rev.,* **31,** 55–71.

——, and H. K. Iyer, 1982: Permutation techniques for analyzing multi-response data from randomized block experiments. *Commun. Stat.,* **A11,** 1427–1437.

Narula, S. C., and J. F. Wellington, 1982: The minimum sum of absolute errors regression: A state of the art survey. *Int. Stat. Rev.,* **50,** 317–326.

Nicholls, N., 1984: Predictability of interannual variations of Australian seasonal tropical cyclone activity. *Mon. Wea. Rev.,* **113,** 1144–1149.

Nicholson, S. E., 1979: Revised rainfall series for the West African subtropics. *Mon. Wea. Rev.,* **107,** 620–623.

——, 1988: Land surface–atmosphere interaction: Physical processes and surface changes and their impact. *Progr. Phys. Geogr.,* **12,** 36–65.

Rey, W. J. J., 1983: *Introduction to Robust and Quasi-Robust Statistical Methods.* Springer-Verlag.

Seneta, E., 1983: The weighted median and multiple regression. *Aust. J. Stat.,* **25,** 370–377.

Shapiro, L. J., 1989: The relationship of the quasi-biennial oscillation to Atlantic tropical storm activity. *Mon. Wea. Rev.,* **117,** 1545–1552.

Sheynin, O. B., 1973: R. J. Boscovich's work on probability. *Arch. Hist. Exact Sci.,* **9,** 306–324.

Simpson, R. H., 1974: The hurricane disaster potential scale. *Weatherwise,* **27,** 169–186.